10 January 1997

ELSEVIER

Chemical Physics Letters 264 (1997) 359–365

CHEMICAL PHYSICS LETTERS

Far infrared transmittance of $Sc_2@C_{84}$ and $Er_2@C_{82}$ [1]

S.M. Grannan [a], J.T. Birmingham [a], P.L. Richards [a], D.S. Bethune [b], M.S. de Vries [b], P.H.M. van Loosdrecht [b,2], H.C. Dorn [c], P. Burbank [c], J. Bailey [c], S. Stevenson [c]

[a] *Department of Physics, and Division of Materials Sciences, Lawrence Berkeley Laboratory, University of California, Berkeley, CA 94720, USA*

[b] *I.B.M. Research Division, Almaden Research Center, 650 Harry Road, San Jose, CA 95120, USA*

[c] *Department of Chemistry, Virginia Polytechnic Institute and State University Blacksburg, VA 24061, USA*

Received 22 April 1996; in final form 24 October 1996

Abstract

We have measured the far infrared transmittance of $Sc_2@C_{84}$ and $Er_2@C_{82}$ at 1.5 K between 30 and 200 cm^{-1}. Both materials are observed to have a large primary absorption feature centered at 95 cm^{-1} with a width of approximately 50 cm^{-1}, as well as a number of secondary absorption features which are different in the two materials. This is the first study of the far infrared properties of metallofullerenes and may help in the determination of the structural and electronic properties of these materials.

1. Introduction

The recently discovered encapsulation of a metal atom or atoms inside fullerene cages [1–3] has excited considerable interest because these materials may have novel properties and applications. However, due to the extreme difficulty in producing purified samples in quantities greater than a few hundred micrograms, characterization of these metallofullerenes has been hampered. Many theoretical questions remain concerning the formation, structure, and electronic properties of these materials [4]. Theoretical calculations [5–9] of the minimum energy configurations for $La@C_{82}$, $La_2@C_{80}$, $Li@C_{60}$, and $Na@C_{60}$ have predicted that a metal atom encapsulated in a fullerene cage typically donates electrons to the cage and assumes a noncentral position. Charge transfer has been confirmed by ESR studies in several materials [10,11] and by XPS measurements [12]. In a theoretical investigation of the properties of $Sc_2@C_{84}$, Nagase and Kobayashi [13] calculated that each Sc atom donates two electrons to the C_{84} cage, and that these four extra electrons are distributed almost uniformly on the cage surface. The two Sc atoms are strongly bound at opposite ends of the C_{84} cage with a separation of ~ 4 Å. This distance is considerably larger than the Sc–Sc separation in the Sc dimer, 2.7 Å, and hence the atoms are expected to interact independently with the cage [14]. The Sc bonding to the fullerene cage was found to be primarily electrostatic and due to polarization. Movements of the charged metal atom or atoms

[1] This work was supported in part by the Director, Office of Energy Research, Office of Basic Energy Sciences, Materials Sciences Division of the U.S. Department of Energy under Contract No. DE-AC03-76SF00098.

[2] Current address: 2. Phys. Institut RWTH Aachen, Templergraben 55, D-52056 Aachen, Germany.

PII S0009-2614(96)01313-9

trapped inside the cage are expected to have large dipole derivatives and produce very strong far infrared transitions, yielding spectra which are extremely sensitive to the size of the cage, the mass and charge of the encapsulated metal atom or atoms, and the potential inside the cage [8]. Thus, a measurement of the far infrared properties of these species may provide an excellent diagnostic of the properties of endohedral carbon cage molecules.

In this Letter we demonstrate two experimental techniques for studying the far infrared transmittance of metallofullerenes which are optimized for the study of very small sample quantities. The first technique involves placing the metallofullerene sample in the middle of a 1.2 mm thick parafilm pellet, which is then cooled to 1.5 K and studied using Fourier transform spectroscopy between 30 and 340 cm^{-1}. Using this technique, we have measured the transmittance spectrum of $Sc_2@C_{84}$ and are able to observe absorption features at the level of one and a half percent. This method allows complete sample recovery. The second technique we have developed is to sublime the metallofullerene sample onto a 1 mm z-cut crystal quartz substrate, which is then cooled to approximately 1.5 K and studied using Fourier transform spectroscopy between 20 and 200 cm^{-1}. Using this technique we have measured the transmittance spectrum of $Er_2@C_{82}$ and are able to observe absorption features at the level of one percent. These two techniques are useful for studying the far infrared transmittance of materials available in powder form. The parafilm technique is easier and allows the transmittance to be measured at higher frequencies. However, the sublimation technique should be used when a uniform film is required provided that the material has adequate thermal stability.

2. Sample preparation

The $Sc_2@C_{84}$ and $Er_2@C_{82}$ samples studied in this work were produced by arc-vaporization in helium of cored carbon electrodes packed with a mixture of graphite and metal or metal oxide [15]. Production efficiency was increased by reversing the arc polarity and 'back-burning' the carbide-rich cathode deposit. Fullerene molecules were extracted from the carbon soot with CS_2, and the separation of $Sc_2@C_{84}$ and $Er_2@C_{82}$ was accomplished using two-stage high performance liquid chromatography (HPLC) [16,17]. Following HPLC, the samples were analyzed using laser desorption/laser ionization mass spectroscopy [18] and were found to consist of at least 98% of the desired metallofullerene species.

In order to measure the far infrared transmittance of $Sc_2@C_{84}$, we placed the material in the middle of a parafilm pellet as outlined below. We first deposited approximately 500 μg of $Sc_2@C_{84}$ dissolved in CS_2 into an 0.3 cm diameter indent on a 120 μm thick parafilm substrate and allowed the solvent to slowly evaporate. This was done in a nitrogen atmosphere to avoid condensation of water onto the substrate. This created a $Sc_2@C_{84}$ disk which measured 0.3 cm in diameter and 40 ± 10 μm in thickness. We then baked the sample in a 60°C oven for 30 min to remove any residual solvent. The parafilm substrate was surrounded by additional parafilm layers and gently compressed between two glass microscope slides. The composite structure was heated to just above the parafilm melting temperature (< 100°C) on a hot plate to produce a solid 1.2 mm thick parafilm pellet. We used the same technique to create a parafilm pellet containing a C_{60} disk measuring 0.3 cm in diameter and 200 ± 20 μm in thickness which we used to confirm the reliability of the measurement technique. In addition we produced three pure parafilm pellets to use as references.

To prepare the $Er_2@C_{82}$ sample, we heated approximately 700 μg of the material to 500°C in a vacuum and sublimed it onto a 1 mm thick z-cut crystal quartz substrate to form a disk approximately 0.4 cm in diameter and 40 ± 10 μm in thickness. For comparison, we used the same technique to evaporate a C_{60} disk of the same dimensions onto another crystal quartz substrate. In addition we used two crystal quartz substrates as references. All crystal quartz substrates were cut from neighboring spots on a large piece of z-cut crystal quartz in order to minimize the differences in thickness and hence the ratio of their Fabry–Perot interference fringes. The crystal quartz and parafilm substrates were chosen to be 1 and 1.2 mm thick, respectively, so that the separation between Fabry–Perot fringes was less than 3 cm^{-1}.

3. Experimental technique

The far infrared transmittance of the samples at 1.5 K was measured with a 1.5 K composite bolometer in conjunction with a Michelson interferometer, using Fourier Transform Spectroscopy [19]. The bolometer uses neutron transmutation [20] doped Ge as the thermometric material. The interferometer was operated in a step-and-integrate mode rather than in a continuous scan mode to improve the noise performance. To measure spectra over an extended frequency region we used several different combinations of beamsplitters and warm filters. The warm filter was selected to remove all radiation at frequencies above the range of study, thus avoiding aliasing effects. The cold 0.001 in. thick black polyethylene filter was chosen to minimize bolometer loading from unchopped radiation.

We determined the transmittance spectrum of the fullerene samples by computing the ratio of the bolometer response when the fullerene sample and substrate were in the light path to the bolometer response when the bare substrate was in the light path. We also examined the ratio of the bolometer responses when two nominally identical substrates were in the light path. The difference between this ratio and unity determined the degree to which our data were contaminated by systematic noise, drifts, and small differences in substrate thickness or composition. For each position of the sample wheel, we obtained a large number of spectra and averaged them in order to minimize the effects of bolometer noise and slow drifts in the bolometer temperature.

4. Experimental results

Due to the very small quantities of sample available, the accuracy of our measurements of the transmittance of $Sc_2@C_{84}$ and $Er_2@C_{82}$ was limited by our ability to match the sample and reference substrates as discussed above. We will first discuss measurements on $Sc_2@C_{84}$ embedded in a 1.2 mm thick parafilm pellet. The transmittance of a reference pellet at 1.5 K is shown in Fig. 1, curve 1. Parafilm has a sharp absorption feature at 77 cm^{-1} and two broad absorption features at 255 and 340 cm^{-1}. In addition, the Fabry Perot interference

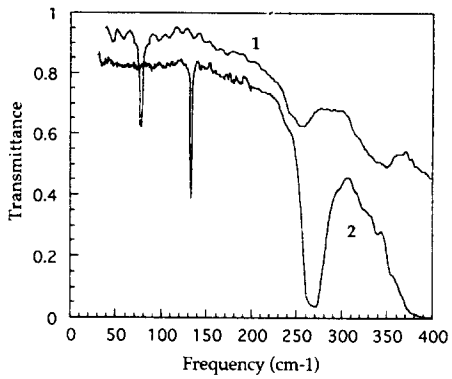

Fig. 1. Transmittance at 1.5 K of a 1.2 mm thick parafilm pellet (curve 1) and a 1 mm thick z-cut crystal quartz substrate (curve 2) between 30 and 400 cm^{-1}.

fringes in the transmittance spectrum of a 1.2 mm thick parafilm pellet are separated by $\Delta f = 1/2nt \approx 2.7$ cm^{-1} where $n \approx 1.56$. The ratio of the spectra of two parafilm reference pellets is shown in Fig. 2, curve 0. This curve has a number of features less than 0.01 in height and less than 5 cm^{-1} in width which are due to the differences in the Fabry Perot interference fringes of the two samples. The broad 3% absorption feature at 260 cm^{-1} arises from the broad parafilm absorption feature at 255 cm^{-1}. These

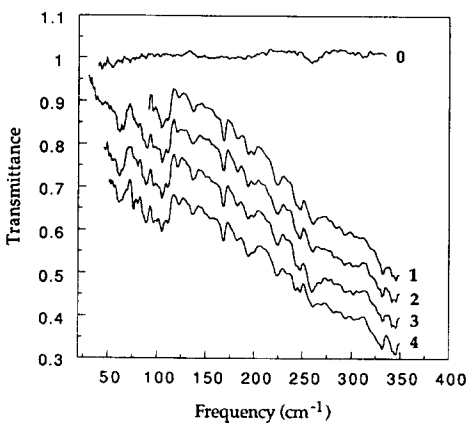

Fig. 2. Transmittance of $Sc_2@C_{84}$, determined by taking the ratio of the $Sc_2@C_{84}$-containing parafilm pellet with: parafilm reference #1 (curve 1); parafilm reference #1 with a different filtering scheme (curve 2); parafilm reference #2 (curve 3); and parafilm reference #3 (curve 4). The curve labelled '0' shows the ratio of parafilm reference #2 to parafilm reference #1. To facilitate comparison, curves 2, 3, and 4 have been offset from curve 1 by −0.1, −0.2, and −0.3, respectively.

features, due to small differences in thickness and composition of the parafilm substrates, are above the noise level of our instrument and practically limit our ability to measure absorption features in $Sc_2@C_{84}$.

The transmittance of $Sc_2@C_{84}$ between 30 and 350 cm^{-1} is plotted in Fig. 2, curves 1 through 4. The four curves were generated by computing the ratio of the $Sc_2@C_{84}$-containing parafilm pellet with: parafilm reference #1 (curve 1); reference #1, measured with a different filtering scheme (curve 2); reference #2 (curve 3); and reference #3 (curve 4). For comparison purposes curves 2, 3, and 4 have been offset from curve 1 by -0.1, -0.2, and -0.3 respectively. The agreement between the four curves is remarkably good, and implies that noise is not important. curve 4 has a small absorption feature at 77 cm^{-1} not observed in curves 1, 2, and 3, which we attribute to imperfect ratioing of the 77 cm^{-1} absorption feature in parafilm. Features smaller than 0.015 cannot be distinguished from differences in the Fabry Perot interference fringes between the sample and reference parafilm pellets. In Fig. 3, curve 1, we plot the absorption coefficient computed from the average of these transmittance spectra. Table 1 summarizes the absorption features observed in $Sc_2@C_{84}$. The most prominent absorption feature

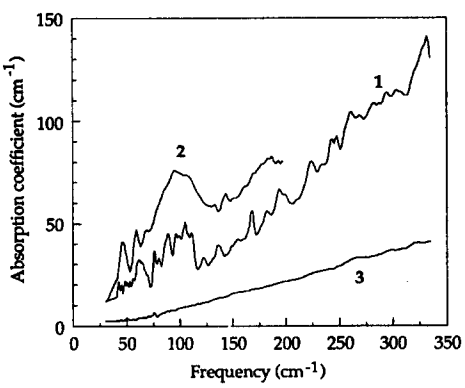

Fig. 3. Absorption coefficient as a function of frequency for $Sc_2@C_{84}$ (curve 1), $Er_2@C_{82}$ (curve 2), and C_{60} (curve 3). The $Er_2@C_{82}$ spectrum was measured with a spectral resolution of 2 cm^{-1}. The $Sc_2@C_{84}$ and C_{60} spectra were measured with a spectral resolution of 1 cm^{-1} below 200 cm^{-1}, and 1.5 cm^{-1} above 200 cm^{-1}. Due to uncertainty in sample thicknesses, curves 1, 2, and 3 are determined to within multiplicative errors of 25, 25 and 10%, respectively.

Table 1
Absorption features in $Sc_2@C_{84}$

Frequency (cm^{-1})	$\Delta\alpha$ (cm^{-1})	Δf (cm^{-1})
62	12	10
76 (pf)	6	3
88	12	10
95	20	40
97	6	8
105	8	7
122	5	8
137	7	10
168	12	10
182	5	8
194	11	14
222	8	12
245	8	10
260 (pf?)	10	20
330 (pf?)	10	10
345 (pf?)	10	10

Columns show the center frequency, height $\Delta\alpha$ relative to the background absorption coefficient, and width Δf. The center frequency is determined to within ± 2 cm^{-1}; we estimate a 10% error in our determination of $\Delta\alpha$ and Δf. Features which are believed to be due to small differences between the sample parafilm pellet and a reference parafilm pellet are marked by (pf).

we observe is a band centered at approximately 95 cm^{-1}, on top of which are superposed a number of smaller, narrower absorption features.

Our measurements of the transmittance of $Er_2@C_{82}$ were also limited by small differences in thickness and composition between the crystal quartz sample substrate and reference substrate. The transmittance of a 1 mm thick z-cut crystal quartz substrate at 1.5 K is shown in Fig. 1, curve 2. Crystal quartz has a sharp absorption feature at 132.5 cm^{-1}. In addition, the Fabry Perot interference fringes in the transmittance spectrum of a 1 mm thick z-cut crystal quartz substrate are separated by $\Delta f = 1/2nt \approx 2.3$ cm^{-1} where $n \approx 2.2$. The ratio of the spectra of two reference crystal quartz substrates has a number of features less than 0.01 in height and less than 3 cm^{-1} in width which are due to the differences in the Fabry Perot interference fringes of the two samples.

We have converted the transmittance spectrum of $Er_2@C_{82}$ into a plot of absorption coefficient as a function of frequency, as shown in Fig. 3, curve 2. All features less than 0.01 in the transmittance spec-

Table 2
Absorption features in $Er_2@C_{82}$

Frequency (cm^{-1})	$\Delta\alpha$ (cm^{-1})	Δf (cm^{-1})
45	17	10
59	13	10
69	7	10
94	34	70
144	6	10
177	5	25

The center frequency is determined to within ± 2 cm^{-1}; we estimate a 10% error in our determination of $\Delta\alpha$ and Δf. Columns show the center frequency, height $\Delta\alpha$ relative to the background absorption coefficient, and width Δf.

trum are attributed to differences in the Fabry Perot interference fringes between the sample and reference substrates. Table 2 summarizes the absorption features observed in $Er_2@C_{82}$, listed in order of increasing frequency. The largest absorption feature we observe is a broad absorption centered at approximately 94 cm^{-1}, similar to the feature observed in $Sc_2@C_{84}$.

We re-measured the transmittance spectrum of the sample after approximately 80% of the sample was removed and again observed the same absorption features; however, the absorption was reduced by a factor of approximately five. This confirms that the observed far-infrared absorption features are intrinsic to the Er_2C_{82}.

For comparison purposes, we also measured the transmittance spectrum of a 200 μm thick C_{60} layer embedded in a parafilm pellet and a 40 μm thick C_{60} film sublimed onto a crystal quartz substrate. Both C_{60} samples had been exposed to air. The frequency dependence of the deduced absorption coefficient of the thicker film is shown in Fig. 3, curve 3. The spectrum of the 40 μm thick C_{60} film was found to be similar. The absorption coefficient is featureless and increases linearly with frequency between 100 and 330 cm^{-1}, in agreement with the result [21] of Onari et al. The small feature at 77 cm^{-1} is an artifact of the 77 cm^{-1} parafilm absorption. Our measured absorption coefficient α at 60 cm^{-1} is 3.9 ± 0.4 cm^{-1} at $T = 1.5$ K, compared to 4.2 cm^{-1} at $T = 4$ K measured by FitzGerald and Sievers [22] in C_{60} which had been exposed to air. Our sample is too thin for us to observe the air-induced impurity bands [22] at 18, 27 and 59 cm^{-1}. The good agreement between our measured C_{60} absorption and that published in the literature, as well as the fact that we do not observe any significant absorption features between 30 and 330 cm^{-1}, confirms the reliability of our sample preparation and measurement techniques.

5. Discussion and conclusion

In discussing the vibrational properties of the metallofullerenes we distinguish between internal and external vibrations. The internal motions involve carbon–carbon and metal–carbon bending and stretching vibrations, whereas the external modes involve translational and rotational motions of the entire cage. Theoretical calculations [23] by Negri et al. of the infrared active vibrational modes of an empty C_{84} cage using the quantum chemical force field for pi electrons (CQFF/PI) method predict a lowest energy band at around 200 cm^{-1}. A similar calculation [24] by Orlandi et al. for an empty C_{82} cage also finds a lowest energy infrared band at around 200 cm^{-1}. In the case of a metallofullerene with a relatively strong metal–cage bonding one expects to measure an experimental spectrum significantly different from these calculations [8]. In particular one also expects modes to appear below 200 cm^{-1}. Even in the case of a weak metal–cage bonding, the charge transfer to the cage will certainly lead to a significant renormalization of the cage frequencies. The spectra presented here show many reproducible absorption features below 300 cm^{-1}. In view of the above discussion, we propose that many of the observed features are due to modified cage vibrations.

Among the internal modes, the metal–cage vibrations are expected to give the strongest contribution to the far infrared spectrum due to their large dipole derivatives. Without knowledge of the bonding strength between the metal atoms and the cage, it is difficult to predict their vibrational frequencies. Since the Er (atomic weight 167.3) is much heavier than the Sc (atomic weight 44.96), one expects the Er–cage vibrations at lower frequencies than the Sc–cage vibrations for comparable bonding to the cage. However, without more knowledge of the metal–cage interaction we cannot yet assign any of the observed absorption modes.

The most striking feature in the spectra of $Sc_2@C_{84}$ and $Er_2@C_{82}$ is the large absorption at 95 cm^{-1} observed in both materials. The coincidence of the 95 cm^{-1} absorption in both materials suggests that the vibration responsible for this feature should be independent of the large mass difference between Er and Sc. The only modes which are relatively insensitive to this mass difference are the external modes. The frequencies of these modes depend on the intermolecular force constants and either the total masses (translations) or total inertial moments (rotations) of the molecules. If we make the reasonable assumption that the force constants are comparable in both materials, we estimate the difference between the external frequencies of both molecules to be about 10% for the translational modes and only 2% for the rotational modes. In view of these small differences, we propose that the 95 cm^{-1} absorption feature is due to an external vibration.

Although this is the first experimental study of the far infrared properties of metallofullerenes, Kikuchi et al. have measured the infrared absorption spectra [25] of C_{82} and LaC_{82} above 400 cm^{-1}. They found approximately ten absorption lines between 400 and 800 cm^{-1} in both samples and some correlation between the LaC_{82} modes and bending motions of the cage. Although some of their absorption features are not clearly distinguishable from the noise, they appear to have typical widths of 10 cm^{-1}, similar to the widths of the absorption features seen in $Sc_2@C_{84}$ and $Er_2@C_{82}$.

Due to the extreme difficulty in producing and purifying metallofullerene samples, we were limited to studying two species of dimetallofullerenes $Sc_2@C_{84}$ and $Er_2@C_{82}$. However, if sample production becomes more efficient, an especially interesting study could be performed on a sequence such as C_{84}, $Sc@C_{84}$, $Sc_2@C_{84}$, and $Sc_3@C_{84}$. As discussed above, the C_{84} cage without inclusions is not expected to show infrared activity below 200 cm^{-1}. If theoretical expectations that the two Sc atoms are essentially noninteracting at opposite ends of the C_{84} cage are correct, $Sc@C_{84}$ and $Sc_2@C_{84}$ would show similar far infrared spectra with the absorption coefficients approximately twice as strong in the dimetallofullerene. $Sc_3@C_{84}$ should show a significantly different transmittance spectrum if the three Sc atoms are enclosed as a trimer which moves relatively freely throughout the C_{84} cage, analogous to the behavior indicated by EPR measurements [26] for Sc_3C_{82}. A systematic study of a variety of cages and metal inclusions will reveal much about the structure and properties of these fascinating new materials.

Acknowledgements

We are indebted to E.E. Haller, J. Emes, and J. Beeman for providing the neutron transmutation doped thermistor and to D. Miller for many useful discussions. This work was supported by the Director, Office of Energy Research, Office of Basic Energy Sciences, Materials Sciences Division of the U.S. Department of Energy under Contract No. DE-AC03-76SF00098. SG was supported by a Department of Education Fellowship. PvL gratefully acknowledges support from the Dutch Organization for Scientific Research (NWO). HCD gratefully acknowledges support for this work from the National Science Foundation.

References

[1] J.R. Heath, S.C. O'Brien, Q. Zhang, Y. Lin, R.F. Curl, H.W. Kroto, F.K. Tittel and R.E. Smalley, J. Am Chem. Soc. 107 (1985) 7779.
[2] Y. Chai, T. Guo, C. Jin, R.E. Haufler, L.P.F. Chibante, J. Fure, L. Wang, J.M. Alford and R.E. Smalley, J. Phys. Chem. 95 (1991) 7564.
[3] R.D. Johnson, M.S. de Vries, J.R. Salem, D.S. Bethune and C.S. Yannoni, Nature 355 (1992) 239.
[4] D.S. Bethune, R.D. Johnson, J.R. Salem, M.S. de Vries and C.S. Yannoni, Nature 366 (1993) 123.
[5] S. Nagase, K. Kobayashi, T. Kato and Y. Achiba, Chem. Phys. Lett. 201 (1993) 475.
[6] K. Kobayashi, S. Nagase and T. Akasaka, Chem. Phys. Lett. 245 (1995) 230.
[7] C.G. Joslin, J. Yang, C.G. Gray, S. Goldman and J.D. Poll, Chem. Phys. Lett. 208 (1993) 86.
[8] G.W. Van Cleef, G.D. Renkes and J.V. Coe, J. Chem. Phys. 98 (1993) 860.
[9] K. Laasonen, W. Andreoni and M. Parrinello, Science 258 (1992) 1916.
[10] S. Bandow, H. Kitagawa, T. Mitani, H. Inokuchi, Y. Saito, H. Yamaguchi, N. Hayashi, H. Sato and H. Shinohara, J. Phys. Chem. 96 (1992) 9609.
[11] H. Shinohara, H. Sato, Y. Saito, M. Ohkohchi and Y. Ando, J. Phys. Chem. 96 (1992) 3571.
[12] J. Weaver, Y. Chai, G. Kroll, C. Jin, T. Ohno, R. Haufler, T. Guo, J. Alford, J. Conceicao, L. Chibante, A. Jain, G. Palmer and R. Smalley, Chem. Phys. Lett. 190 (1992) 460.

[13] S. Nagase and K. Kobayashi, Chem. Phys. Lett. 231 (1994) 319.
[14] J. Harris and R.O. Jones, J. Chem. Phys. 70 (1979) 830.
[15] R. Beyers, C-H. Kiang, R.D. Johnson, J.R. Salem, M.S. de Vries, C.S. Yannoni, D.S. Bethune, H.C. Dorn, P. Burbank, K. Harich and S. Stevenson, Nature 370 (1994) 196.
[16] S. Stevenson, H.C. Dorn, P. Burbank, K. Harich, Z. Sun, C. Kiang, J.R. Salem, M.S. de Vries, P. van Loosdrecht, R. Johnson, C. Yannoni, and D. Bethune, Anal. Chem. 66 (1994) 2680.
[17] S. Stevenson, H.C. Dorn, P. Burbank, K. Harich, J. Haynes, C. Kiang, J.R. Salem, M.S. de Vries, P. van Loosdrecht, R. Johnson, C. Yannoni, and D. Bethune, Anal. Chem. 66 (1994) 2675.
[18] G. Meijer, M.S. de Vries, H.E. Hunziker, and H.R. Wendt, Appl. Phys. B 51 (1990) 395.
[19] D. Miller, P.L. Richards, S. Etemad, A. Inam, T. Venkatesan, B. Dutta and X.D. Wu, Phys. Rev. B 47 (1993) 8076.
[20] E.E. Haller, N.P. Palaio, M. Rodder, W.L. Hansen and E. Kreysa, in: Neutron Transmutation Doping of Semiconductor Materials, ed. R.D. Larrabee (Plenum Press, New York, 1984), p. 21.
[21] S. Onari, K. Tada and T. Arai, J. Phys. Soc. Jap. 60 (1991) 4392.
[22] S.A. Fitzgerald and A.J. Sievers, J. Chem. Phys. 101 (1994) 7283.
[23] F. Negri, G. Orlandi and F. Zerbetto, Chem. Phys. Lett. 189 (1992) 495.
[24] G. Orlandi, F. Zerbetto and P.W. Fowler, J. Phys. Chem. 97 (1993) 13575.
[25] K. Kikuchi, S. Suzuki, Y. Nakao, N. Nakahara, T. Wakabayashi, H. Shiromaru, K. Saito, I. Ikemoto and Y. Achiba, Chem. Phys. Lett. 216 (1993) 67.
[26] P.H.M. van Loosdrecht, R.D. Johnson, M.S. De Vries, C.-H. Kiang, D.S. Bethune, H.C. Dorn, P. Burbank and S. Stevenson, Phys. Rev. Lett. 73 (1994) 3415.